

## Chapter II. Objectives

The main objective of this Ph.D. Thesis work is to investigate the physicochemical properties of the main phospholipids that constitute the inner membrane of the mitochondrion and to investigate if there is a specific interaction of *cyt c* with some particular phospholipid. Two model membranes have been used: the one-dimensional (monolayers) and the vesicular model membrane (micelles and liposomes). To mimic the inner membrane of mitochondria three main phospholipids, POPE, POPC and CL, have been used.

The specific objectives of this work are:

- To investigate the stability of binary mixtures of phospholipids in order to know the more thermodynamically stable compositions.
- To study the different mechanism of interaction of *cyt c* with monolayers.
- To characterize the topographic characteristics of the monolayers of interest by using the Langmuir-Blodgett technique and atomic force microscopy.
- To study the variation of surface potential originated by the interaction of *cyt c* adsorption on liposomes.
- To form supported planar bilayers to investigate the existence of laterally segregated phospholipids domains by atomic force microscopy.
- To investigate if there is a selective adsorption of *cyt c* for some phospholipid domains.



## Chapter III. Materials

### III.1. PHOSPHOLIPIDS

1-Palmitoyl-2-Oleoyl-*sn*-Glycero-3-Phosphocholine (POPC), 1-Palmitoyl-2-Oleoyl-*sn*-Glycero-3-Phosphoethanolamine (POPE), 1-Palmitoyl-2-Oleoyl-*sn*-Glycero-3-[Phospho-*rac*-(1-glycerol)] (POPG) and cardiolipin (CL) were purchased to Avanti Polar Lipids, Inc, (Alabaster, AL, USA).

### III.2. *CYT C*

*Cyt c* from horse heart was purchased to Sigma-Aldrich (St. Louis, MO, USA).

### III.3. FLUORESCENT PROBES

8-anilino-1-naphthalenesulfonic acid (ANS) and 1,6-Diphenyl-1,3,5-hexatriene (DPH) were purchased to Sigma-Aldrich (St. Louis, MO, USA).

### III.4. FILTERS

Four different filters were purchased to Nucleopore<sup>®</sup> (Costar Scientific Corporation, MA, USA)

- Filters with pore diameter of 200 nm of polycarbonate.
- Filters with pore diameter of 400 nm of polycarbonate.
- Filters with pore diameter of 450 nm of nylon.
- Spacers for polycarbonate membranes (Drain disc).

### III.5. SOLID SUPPORTS

Solid support to LB films extraction and SPBs adsorption was muscovite mica. It was purchased to Asheville-Schoonmaker Mica Co. (Newport News, VA, USA). Its chemical composition, less water of constitution, is  $H_2KAl_3(SO_4)_3$ . Its specific properties are summarized in Table VI.

**Table VI.** Properties of the muscovite mica.

<b>Mica Properties</b>	
Thermal conductivity	$16 \times 10^{-4}$ Cal/Cm <sup>2</sup> /Sec/Cm/°C
Specific gravity	2.6 to 3.2 (average 2.83)
Specific heat	0.207
Moh hardness scale	2.8 to 3.2
Shore hardness	80 to 150
Optical Axial Angle	50 to 75 degrees
Volume resistivity	$2 \times 10^{13}$ to $1 \times 10^{17}$ ohms/cm <sup>3</sup>
*Dielectric Strength (1 to 3 mils thick in air)	3000 to 6000 volts/Mil
Dielectric Constant	6.5 to 8.7
Power Factor (1/0)	0.0001 - 0.0004
Maximum Coefficient of Expansion	0.000036 per °C
Modulus of Elasticity (10 mils thick)	About $25 \times 10^6$ lb./sq. in
Water of Constitution	4.5 Percent
Water of Constitution, driven off at	600 to 800 °C
Maximum Temperature of Use	600 °C

\*The lower the thickness, the greater the dielectric strength per mil.

### III.6. AFM CANTILEVERS

Two kinds of cantilevers were used, one kind to scan samples in air and another to scan samples under aqueous solution.

### III.6.1. Cantilevers for samples imaged in air

Cantilevers used in air were purchased from Olympus Optical Co. Ltd., Japan. Cantilevers reference was OMCL-AC160TS. Its specifications are summarized in Table VII.

**Table VII.** Specifications of cantilevers used to scan samples in air.

Properties		Typical values
Tip	Shape	Sharpened Tetrahedral (tilted)
	Height	11 $\mu\text{m}$
	Radius diameter	Smaller than 10 nm
	Angle	Less than 35 degrees
	Material	Single crystal silicon (semiconductor, N type, 4 – 6 $\Omega\cdot\text{cm}$ )
Lever	Shape	Rectangular
	Thickness	4.6 $\mu\text{m}$
	Length	160 $\mu\text{m}$
	Width	50 $\mu\text{m}$
	Spring constant	42 N/m (12-103)
	Resonant frequency	300 kHz (200-400)
	Coating	100 nm aluminum film

Figure 21 shows the cantilever and the chip that contains the tip.

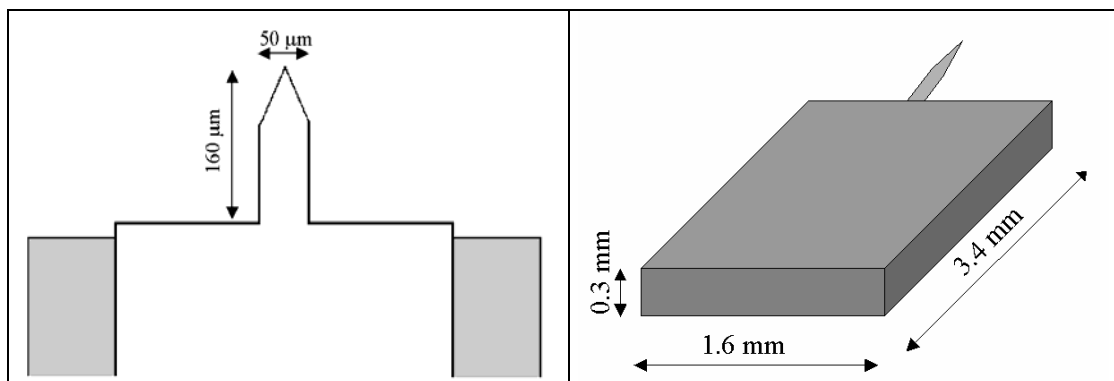


**Figure 21.** Sizes and shapes of the cantilevers and the chips used in air.

### III.6.2. Cantilevers for samples imaged in liquid

Cantilevers used in liquid were purchased from Olympus Optical Co. Ltd., Japan. Cantilevers reference was OMCL-TR400PSA. Its specifications are summarized in Table VIII.

**Table VIII.** Specifications of cantilevers used to scan samples in liquid.

Properties		Typical values	
Tip	Shape	Pyramidal	
	Height	2.9 $\mu\text{m}$	
	Radius diameter	Smaller than 20 nm	
	Material	Silicon nitride	
Lever	Shape	Triangular	
	Thickness	0.4 $\mu\text{m}$	
	Length	200 $\mu\text{m}$	100 $\mu\text{m}$
	Width	166 nm	106 nm
	Spring constant	0.02 N/m	0.08 N/m
	Resonant frequency	11 kHz	34 kHz
	Coating	60 nm of aurum film	

Figure 22 shows the cantilever and the chip that contents the tips.

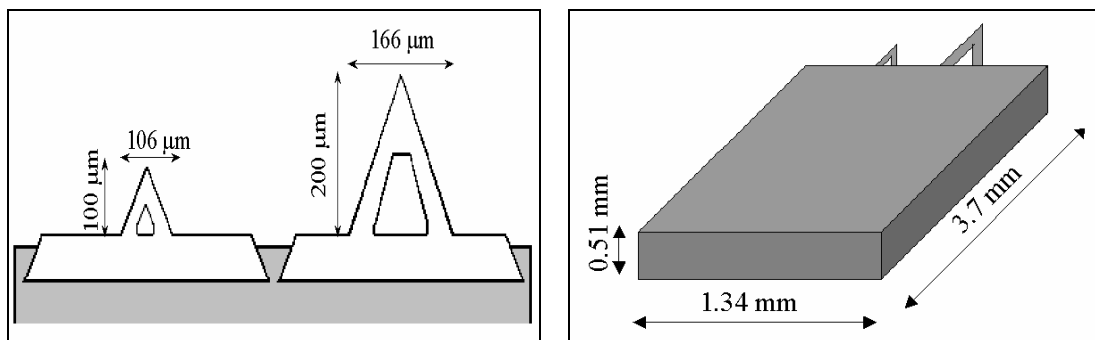


**Figure 22.** Sizes and shapes of the cantilevers and the chips used under liquid environment.

### III.7. REACTIVES AND PRODUCTS

Sodium chloride, Tris hydrochloride (TRIZMA<sup>®</sup>·HCl), calcium chloride, HEPES, ... were purchased to Sigma-Aldrich (St. Louis, MO, USA) with a minimum quality of 99.9 %.

Sulfuric acid 96 %, hydrogen peroxide 30%, methanols, chloroform ... all of analytic qualities were purchased to Sigma-Aldrich (St. Louis, MO, USA).

### III.8. LABORATORY MATERIAL

Usual laboratory material was used: graduated cylinders, volumetric flasks, graduated beakers, Pyrex<sup>®</sup> flasks, Kitasato system (suction flask) ... as well as material of common use: Kimwipes<sup>®</sup> wipers, Eppendorf tubes, Pasteur pipettes, latex and polythene gloves ...

Water used in this work was bidistilled water for monolayers experiments and MiliQ (Millipore<sup>®</sup>) water for fluorescence and AFM experiments.

Semi Micro cuvettes for fluorescence experiments were acquired to Hellma<sup>®</sup> Hispania (Badalona, Spain).

### III.9. INSTRUMENTATION

- Water bidistiller Aquatron A8S from J. Bibby Science Products Limited (Stone, UK).
- Ultra pure water system MilliQ PLUS 185 Millipore (Billerica, MA, USA) equipped with QPACK<sup>®</sup> 1 filters.
- PTFE trough model 312 DMC manufactured by NIMA Technology Ltd (Coventry, UK). This model incorporates two PTFE mobile barriers, one balance and one dipper.
- Vibration-isolated table was purchased to Newport (Irvine, CA, USA).
- Haake cryostat (Karlsruhe, Germany), model D8/G with precision of 0.1 °C.

- Spectrofluorimeter SLM-AMINCO® (Rochester, NY, USA), model 8100 with excitation and emission splits of 8/8 and 4/4 nm/nm, respectively. Spectrofluorimeter was equipped with a XBO 450W/2 OFR lamp from OSRAM.
- Haake cryostat (Karlsruhe, Germany), model DC5/K20 with precision of de 0.1 °C.
- Extruder device from Lipex Biomembranes (Vancouver, BC, Canada).
- Photon correlation spectrophotometer from Autosizer IIc (Malvern Instruments, UK).
- Multimode Atomic Force Mmicroscope III from Digital Instruments® (Santa Barbara, CA, USA) with Nanoscope IV electronics.
- Crison pHmeter (Barcelona, Spain).

### III.10. SOFTWARE

During the performance of this work several software were used:

- ✓ Adobe Acrobat 5.0
- ✓ Adobe Photoshop 5.0
- ✓ Adobe Reader 7.0
- ✓ Excel 2003
- ✓ Internet Explorer 6.0
- ✓ Nanoscope III 5.12r3
- ✓ Origin 6.0
- ✓ Power Point 2003
- ✓ RasMol 2.7.2.1.1
- ✓ Word 2003





## Chapter IV. Experimental Methods

### IV.1. SAMPLES PREPARATION

All samples used during the performance of this work were composed of 4 pure synthetic phospholipids and mixtures of them.

#### IV.1.1. Phospholipids

##### IV.1.1.1. POPC

1-Palmitoyl-2-Oleoyl-*sn*-Glycero-3-Phosphocholine (POPC), 16:0-18:1 PC, is a zwitterionic phospholipid. Two different hydrocarbon chains constitute the hydrophobic region. One hydrocarbon chain in position 1 with 16 carbon atoms and without unsaturations. The other chain is in position 2 with 18 carbon atoms and one unsaturation. A phosphocholine head group forms the hydrophilic region. Its molecular weight is 760.09 g/mol with a transition temperature ( $T_m$ ) of pure phospholipid of  $-2$  °C. Figure 23 shows the structure of POPE.

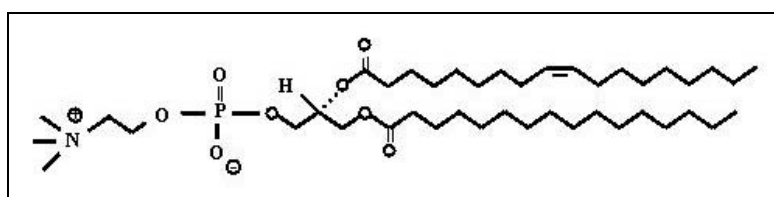


Figure 23. POPC schematic structure.

##### IV.1.1.2. POPE

1-Palmitoyl-2-Oleoyl-*sn*-Glycero-3-Phosphoethanolamine (POPE), 16:0-18:1 PE, is a zwitterionic phospholipid. Two different hydrocarbon chains constitute the hydrophobic region. One hydrocarbon chain in position 1 with 16 carbon atoms and without unsaturations. The other chain is in position 2 with 18 carbon atoms and one unsaturation. A phosphoethanolamine head group forms the hydrophilic region. Its

molecular weight is 718.09 g/mol with a  $T_m$  value of pure phospholipid of 25 °C. Figure 24 shows the structure of POPE.

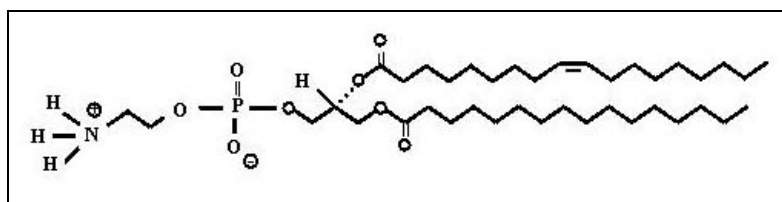


Figure 24. POPE schematic structure.

#### IV.1.1.3. POPG

1-Palmitoyl-2-Oleoyl-*sn*-Glycero-3-[Phospho-*rac*-(1-glycerol)] (POPG), 16:0-18:1 PG, is a phospholipid with a negative net charge. Two different hydrocarbon chains constitute the hydrophobic region. One hydrocarbon chain in position 1 with 16 carbon atoms and without unsaturations. The other one is in position 2 with 18 carbon atoms and one unsaturation. A phosphoglycerol head group forms the hydrophilic region. Its molecular weight is 771.00 g/mol with a  $T_m$  value of pure phospholipid of - 2 °C. Figure 25 shows the structure of the POPG.

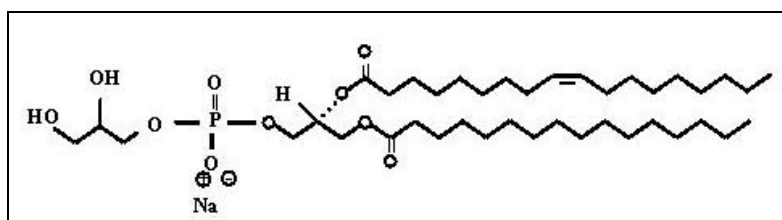


Figure 25. POPG schematic structure.

#### IV.1.1.4. Cardiolpin

Cardiolipin (CL) is not a usual phospholipid. Its structure is similar to two phospholipids linked by its polar regions. It could be identified as two PG molecules, so it presents negative net charge. Figure 26 shows the structure of CL.

CL is not synthetic; it is obtained from heart tissue extraction. There are many kinds of CLs in the sample. CL used in this work presents 86.6 % of 18:2, 8.2 % of 18:1, 1.6 % of 16:1, 1.0 % of 18:3 and 3.6 % of minority structures (results expressed as area

percentage by FAME – GC/FID). Its molecular weight is 1493.92 g/mol with  $T_m$  value of 19 °C.

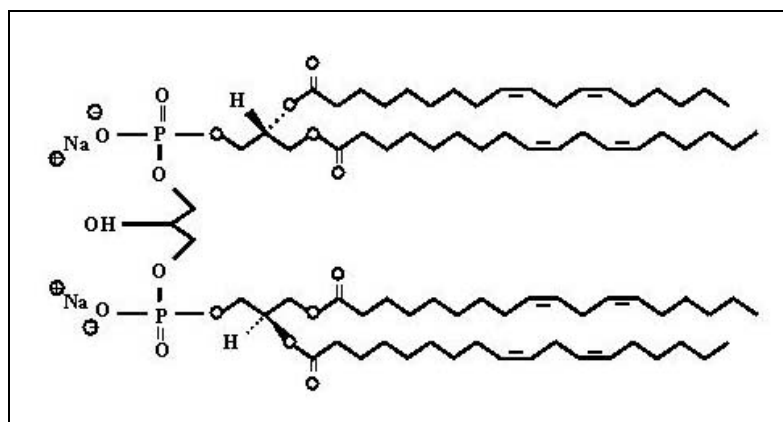


Figure 26. CL schematic structure.

#### IV.1.2. Samples for monolayer and LB films experiments

Phospholipid stock solutions were prepared at 1 mg/mL in chloroform:methanol (3:1, v/v). Aliquots of 50  $\mu$ L were distributed in Eppendorf tubes and the corresponding volume to perform the desired monolayer was taken from these tubes. Errors due to volume evaporation would be the same in all the experiments. Always remaining lipid in the Eppendorf was thrown out.

#### IV.1.3. Samples for fluorescence experiments

Phospholipid stock solutions were prepared at 1 mM in chloroform:methanol (3:1, v/v). From these solutions it was taken enough volume to obtain the desired final concentration of liposomes and placed in a round bottom flask. Solvent was evaporated under a stream of nitrogen obtaining a homogeneous dry phospholipid film at the bottom of the flask. Phospholipid film was maintained under reduced pressure for at least 12 h to remove solvent residues. After that, lipid film was hydrated in 50 mM Tris-HCl, 150 mM NaCl, pH 7.40 to a final concentration of 60  $\mu$ M. Hydration was performed in a cyclic process of vortexing and heating above  $T_m$  of the phospholipids that compound the sample. After this process liposomes were present in the aqueous solution, but their diameters were very scattered (usual values from 100 nm to 1  $\mu$ m).

To minimize possible effects produced by different radii of curvature of the liposomes, they were extruded 10 times through two polycarbonate filters (200 nm pore size) with an Extruder device. Then, unilamellar vesicles of 200 nm of diameter were formed in the aqueous solution. Liposome diameter values were checked with the light scattering technique showing a pronounced pick around 200 nm with satisfactory polydispersity ( $< 0.10$ ). Liposome sample was used after overnight stabilization at room temperature.

Liposome concentration in the sample was checked with a colorimetric method performed by Stewart [Stewart, 1980]. Final liposome concentration in the sample was 50  $\mu\text{M}$  of phospholipid.

#### IV.1.4. Samples for NMR and DSC experiments

Suspensions were obtained by hydration the sample in 50 mM Tris·HCl, 150 mM NaCl, buffer pH 7.40 and with or without 20 mM  $\text{CaCl}_2$ , to a final concentration of 2.5 mM. For  $^{31}\text{P}$ -Nuclear Magnetic Resonance ( $^{31}\text{P}$ -NMR) spectroscopy experiments, the resulting suspension was then pelleted by ultracentrifugation at 115,000  $\times g$  for 1 h at 5°C. The hydrated pellet was then resuspended in 300  $\mu\text{L}$  of supernatant and placed in a conventional 5 mm NMR tube. A capillary tube containing  $\text{D}_2\text{O}$  was added for field-frequency stabilization.

#### IV.1.5. Samples for AFM experiments

Process of liposome formation was the same described in section IV.1.3., but lipid was hydrated in Resuspension Buffer (RB) 20 mM HEPES, 150 mM NaCl, 20 mM  $\text{CaCl}_2$  at pH 7.40 and filters used in the extrusion process were of 400 nm of diameter. Final lipid concentration after extrusion was 250  $\mu\text{M}$ . Vesicle diameter values were checked with the light scattering technique showing a pronounced pick around 400 nm with satisfactory polydispersity ( $< 0.15$ ). The sample was used after overnight stabilization at room temperature.

## IV.2. LANGMUIR-BLODGETTRY

### IV.2.1. Instrumentation

System to obtain monolayers and LB films is represented in Figure 27.

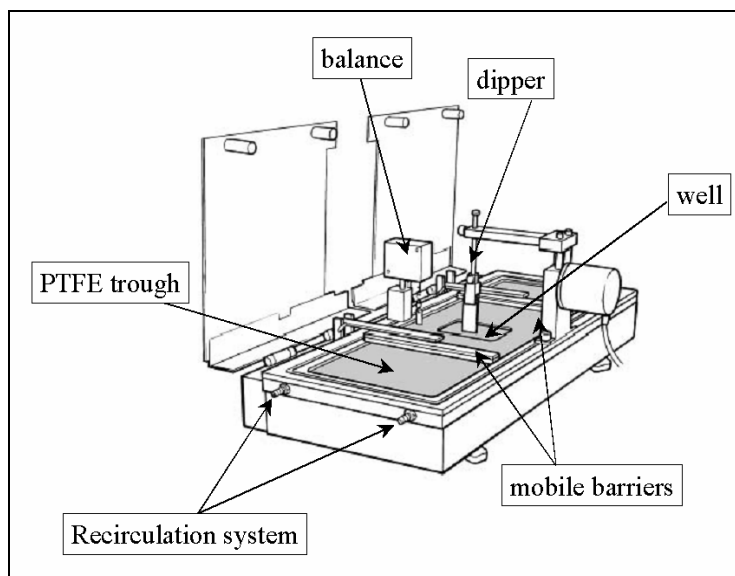


**Figure 27.** PTFE trough and accessories.

Its physical characteristics are summarized in Table IX:

**Table IX.** Physic characteristics of the LB trough used.

<b>Characteristics</b>	
	30 x 10 x 0.4 cm <sup>3</sup>
Trough:	2 compartments of 150 cm <sup>2</sup> well of 25 mm depth and 25 x 30 mm of section
Barriers:	2 independent barriers Symmetric and antisymmetric displacement $v_{\max} : 198 \text{ cm}^2 \cdot \text{min}^{-1}$ $v_{\min} : 2 \text{ cm}^2 \cdot \text{min}^{-1}$
Dipper:	$v_{\max} : 45 \text{ cm}^2 \cdot \text{min}^{-1}$ $v_{\min} : 1 \text{ mm} \cdot \text{min}^{-1}$

The trough is placed on a vibration-isolated table (Figure 28).



**Figure 28.** Vibration-isolated table.

Its physical characteristics are summarized in Table X.

**Table X.** Physical characteristics of the vibration-isolated table.

Vertical		Horizontal		Maximum weight (Kg)	Precision (mm)
Res (Hz)	10 Hz (%)	Res (Hz)	10 Hz (%)		
3.2	90	3.6	96	27	0.6

An air compression pump is attached to the vibration-isolate table. So, the position of the table can be modified actively by three contact points between the table and the surface where it is located. Air compression pump is placed in a different surface than the vibration-isolate table to minimize external noises.

Over the trough it is placed an environment chamber. This chamber has a frontal gate to operate the instrument easily. Environment control provides a major cleanliness of the trough. An external recirculation water bath allows the temperature control of the liquid in the trough. This bath, as the pump, is in a different surface than the trough to minimize external noises.

#### IV.2.2. Surface pressure determination

Surface pressure was determinate with the *Wilhelmy plate* technique. A sheet of chromatographic paper (Chr 1 of Whatman) is hanged from a balance. Plate characteristics are reflected in Figure 29.

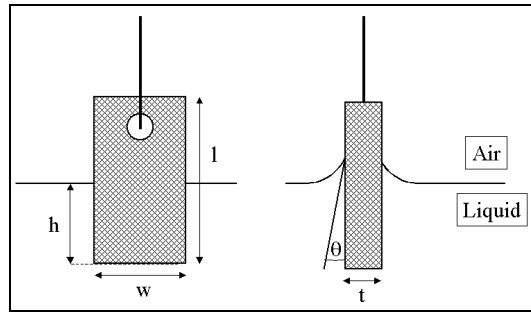


**Figure 29.** Chromatographic paper plate characteristics

where  $h$  is the depth,  $l$  the length,  $w$  the width,  $t$  the thickness and  $\theta$  the contact angle. Surface pressure can be determined if a force balance is carried out on the plate. In this force balance 3 terms may be considered: weight, upthrust and surface tension. These three terms are presented in equation II.

$$F = (\rho_{plate} lwt) \cdot g - (\rho_{liquid} hwt) \cdot g + 2 \cdot (w + t) \cdot \gamma \cdot \cos \theta \quad (II)$$

where  $\rho_{plate}$  is the density of the plate,  $\rho_{liquid}$  is the density of the liquid,  $g$  the gravity acceleration and  $\gamma$  the surface tension of the liquid. This equation can be simplified:

- weight force component can be erased if the pressure reading in the balance is zeroed.
- upthrust force term can be eliminated if the plate is always at the same depth. The plate is always hanged from the balance at the same distance and changes the balance measure but not the depth.
- using paper plates ensures a contact angle near 0 degrees.

Then, equation II can be expressed as:

$$\pi = \Delta\gamma = \frac{\Delta F}{2(w + t)} \quad (III)$$

where surface pressure is in  $\text{mN} \cdot \text{m}^{-1}$  if the force is in mN and perimeter in meters.

### IV.2.3. Phospholipid isotherms

Phospholipid isotherms can give information of the physical state of the molecules that form the monolayer at controlled temperature. Isotherms are acquired compressing laterally the monolayer at a constant velocity while the surface pressure is monitored. A typical schematic representation is shown in Figure 30.

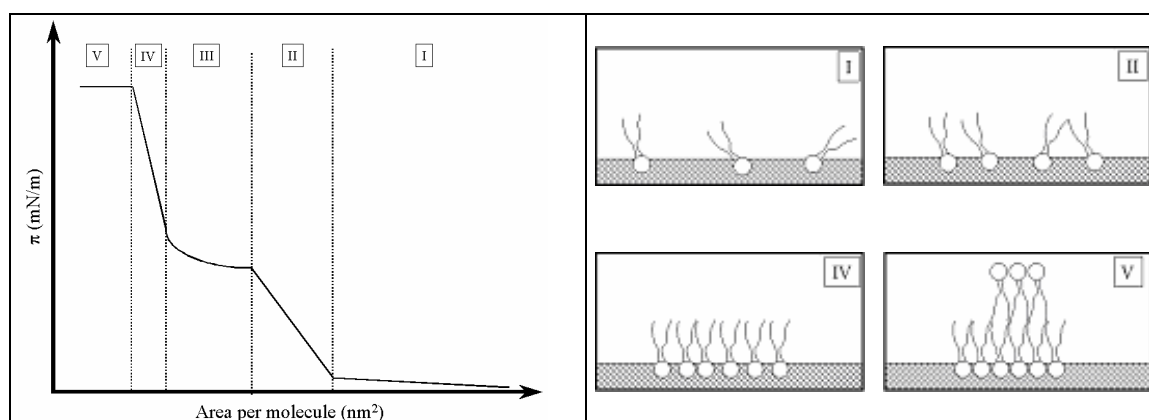


**Figure 30.** Schematic representation of an isotherm. Cartoons show the molecular organization of the phospholipid molecules at the different stages.

Any isotherm presents different stages:

- Stage I: In this stage the monolayer is in a gaseous phase. Molecules interact few with others. Surface pressure increase is small.
- Stage II: Monolayer is in a liquid phase (liquid expanded). Molecules interact more with others. Surface pressure increase is greater than in stage I, as can be seen from the slope in the Figure 30.
- Stage III: Monolayer is going through a phase change. During the phase change, area per molecule is diminished without significant increase of surface pressure. This phase change is towards a more solid phase (liquid condensed).
- Stage IV: In this stage, the condensed phase is compacted. Interaction between molecules is much more intensive than in others stages.

Stage V: Lateral pressure is too much for monolayer stability. Surface pressure reaches the collapse surface pressure and material is sent out towards the bulk liquid phase or to form bilayers. This send out from the interface can be gradually and the slope would be zero or it can be sequentially and the slope would be random.

In this isotherm scheme it has been represented five stages but depending on the phospholipid nature and the environment conditions more or less stages can appear. Number of stages is very dependent on the temperature of the experiment.

#### IV.2.4. Monolayer mathematical analysis

An easy way to process the information from monolayers is to consider the phospholipid molecules as an ideal gas in two dimensions. Deviations from this ideal behavior can show up information of the interaction between molecules. Under these conditions, the pressure is the surface pressure, and the volume is the area per molecule.

##### IV.2.4.1. Ideal and excess area

An ideal gas, in two dimensions, would occupy all the possible area, so two ideal gases would occupy all the possible area, too. Then the ideal area,  $A_{id}$  can be defined as

$$A_{id} = \chi_1 A_1 + \chi_2 A_2 \quad (IV)$$

where  $A_i$  and  $\chi_i$  are the area per molecule and molar fraction of pure component  $i$ , respectively. This equation will be accomplished, in monolayers, in two different cases:

- if phospholipids molecules are behaved as ideal gases and mix up as such.
- if the different phospholipids are absolutely immiscible. So each type of phospholipid would occupy their proportional area without interaction with the other kind of phospholipid.

If one of these conditions is accomplished in an isotherm, values of ideal area as a function of the molar fraction would be aligned in a straight line. This straight line would come from the area per molecule of one pure component towards the area per molecule of the other pure component. Deviations up or down from this straight line would be caused by repulsion or attraction between molecules in the monolayer, respectively.

Another way to observe this behavior is the excess area,  $A^E$ . Excess area represents the ideality degree of the mixture and can be expressed as

$$A^E = A_{12} - \chi_1 A_1 - \chi_2 A_2 \quad (\text{V})$$

where  $A_{12}$  is the area per molecule of the mixed monolayer.

As in the case of ideal area, if one of the cases mentioned above is accomplished, the excess area values as a function of the molar fraction were aligned in a straight line without slope and centered in the zero value. Deviations of ideality would result in positive or negative values of  $A^E$ . Positive values represent that intramolecular repulsion forces exist in the monolayer while negative values represent attractive forces between molecules.

#### IV.2.4.2. Excess and mixing Gibbs energies

Interactions between two different phospholipid molecules in monolayers, at a surface pressure  $\pi$  and a constant temperature  $T$ , can be evaluated from the Gibbs excess energy,  $G^E$ . Gibbs excess energy can be evaluated from:

$$G^E = \int_0^\pi (A_{12} - \chi_1 A_1 - \chi_2 A_2) d\pi = \int_0^\pi A^E d\pi \quad (\text{VI})$$

If the behavior of phospholipid molecules is the ideal gas behavior, Gibbs excess energy would be zero. As in the case of excess area, positive values represent instability

(repulsion forces) while negatives values represents stability (attractive forces between molecules).

A mathematical expression related to Gibbs excess energy is the Gibbs energy of mixing,  $\Delta_{mix}G$ .

$$\Delta_{mix}G = \Delta_{mix}G^{id} + G^E \quad (VII)$$

where  $\Delta_{mix}G^{id}$  is the ideal Gibbs energy of mixing and can be calculated from:

$$\Delta_{mix}G^{id} = RT \cdot (\chi_1 \ln \chi_1 + \chi_2 \ln \chi_2) \quad (VIII)$$

where  $R$  and  $T$  are the universal gas constant and the temperature, respectively.

As in the previous case,  $\Delta_{mix}G$  positive values represent instability (repulsion forces) while negatives values represent stability (attractive forces between molecules).

#### IV.2.4.3. Compressibility modulus

Compressibility modulus,  $C_s$ , is defined at a surface pressure  $\pi$  as:

$$C_s = -\frac{1}{A_\pi} \cdot \frac{dA}{d\pi} \quad (IX)$$

where  $A_\pi$  is the area per molecule at the surface pressure  $\pi$  and  $dA/d\pi$  can be evaluated as the inverse of the slope at the  $(A_\pi, \pi)$  point.

Compressibility modulus provides information of the lateral compression of the monolayer. The higher the values of the compressibility modulus, the lower the energy needed to compress the monolayer a surface pressure differential. So, low  $C_s$  values indicate that it is more difficult to compress the monolayer than at  $C_s$  high values.

### IV.2.5. Subphase buffer

Buffer used as a subphase to carry out isotherms and LB films extraction was formed by:

50 mM TRIS·HCl	7.880 g/L
150 mM NaCl	8.766 g/L
Bidistilled water	enough to 1 L

Solution pH was established in 7.40 and measured with a commercial pHmeter. It was regulated with chlorhydric acid and sodium hydroxide. Resultant buffer was filtered through a Kitasato system with filters of 450 nm of diameter of pore to remove contaminants. Buffer solution was made and immediately used and never stored.

### IV.2.6. Cyt c solution for monolayers

Cyt *c* was resuspended in a glass tube in the same buffer used in the monolayers to a final concentration of 5 mg/mL. This tube was always kept at 4 °C and protected from light.

### IV.2.7. Isotherms performance

Previous to start the experiment the cleanness of the subphase was assured. It was needed times of 15 minutes to allow the solvent evaporation. Then isotherm was acquired compressing the monolayer at a constant rate of 5 cm<sup>2</sup>/min. Due to the plate was made of paper, lipidic material was still at the top of the plate when the first monolayer was ended and aspired. To minimize this effect the first isotherm was not taken into account due to the material that rested in the plate overestimates the calculus of the area per molecule of the first isotherm. Then a minimum of six repetitions for each isotherm was needed to assure the correct feature of the desired isotherm.

#### IV.2.8. LB film extraction

After spreading the phospholipid 15 minutes were needed to solvent evaporation. Then a pressure control to the desired surface pressure was acquired with a lateral compression of  $5 \text{ cm}^2/\text{min}$ . When the surface pressure was reached the electronic device controls the barrier position to keep constant the surface pressure between barriers. Times greater than 30 minutes were needed to obtain a stable monolayer. After that, dipper was lifted/immersed at a constant velocity of  $1 \text{ mm}/\text{min}$ . During the extraction, barrier positions were automatically adjusted to keep the surface pressure constant between them.

#### IV.2.9. Cyt c adsorption isotherms

Phospholipid monolayer was performed as described in section IV.2.7. with an injection port placed in the edge (Figure 31). This port allows a very shallow angle of insertion and allows the injectant to be injected at the center of the trough. Then monolayer was compressed to the desired surface pressure and *cyt c* aliquot can be injected under it through the injection port. A magnet was introduced at the bottom of the trough and was on continuous stirring to homogenize the subphase.

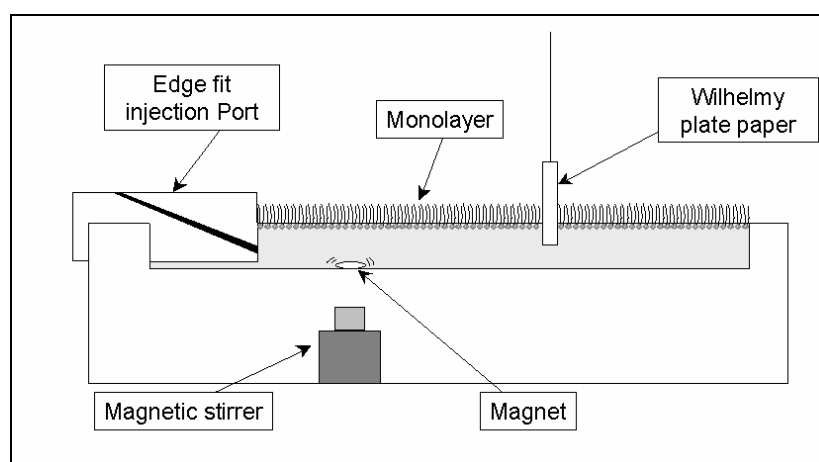


**Figure 31.** Schematic representation of the trough during *cyt c* injection under the lipid monolayer.

Collected data was processed and adjusted to a modified Langmuir isotherm:

$$\Delta A = \Delta A_{\max} \frac{(kt)^b}{1 + (kt)^b} \quad (\text{X})$$

where  $\Delta A_{\max}$  is the maximum value of the increment of the area per molecule,  $k$  is the process constant and  $b$  is a parameter related to cooperativity of the process.

### IV.3. FLUORESCENCE

#### IV.3.1. Binding experiments

8-anilino-1-naphtalene sulfonic acid was used to determine the membrane surface potential of liposomes of different membrane compositions. Its molecular structure is represented in Figure 32.

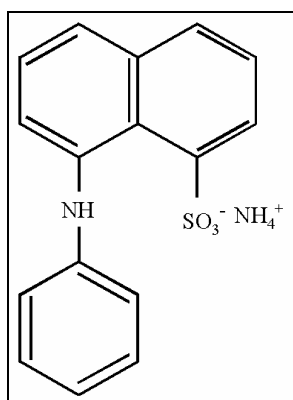


**Figure 32.** ANS molecular structure.

ANS is a fluorescence probe that is nearly non fluorescent in aqueous solution. ANS becomes fluorescence when it is bound to lipid membranes. It is a surface fluorescent probe linked superficially and it is very sensitive to superficial charges present in its neighborhood. ANS presents an excitation wavelength of 380 nm and emission wavelength of 480 nm.

ANS was dissolved in a glass tube with methanol to a final concentration of 5 mM. From this stock solution it was prepared aliquots of 150  $\mu\text{L}$  in Eppendorf tubes before use.

#### IV.3.1.1. Determination of the ANS bound fraction in lipids

Fraction of bound ANS was calculated using equation XI:

$$[ANS]_b = \frac{F_b - F_0}{A_b - A_0} \quad (XI)$$

where  $F_b$  and  $F_0$  are the fluorescence intensities of ANS with and without lipid in the cuvette and  $A_b$  and  $A_0$  are the emission coefficients of ANS in presence and absence of lipid, respectively. Emission coefficients in presence of lipid were determined as the slope in the graphic representation of the fluorescence emission intensity at high lipid concentration (1-2 mM) as a function of low ANS concentration (0.1-1  $\mu$ M) [Ma et al., 1985].

#### IV.3.1.2. Mathematical analysis of the ANS fluorescence

Concentration of bound ANS was represented as a function of the concentration of the free ANS calculated according equation XII.

$$[ANS]_{Total} = [ANS]_b + [ANS]_{Free} \quad (XII)$$

and adjusted to a Langmuir isotherm equation (eq. XIII):

$$[ANS]_b = \sum_{i=1}^n C_i \frac{(k_i [ANS]_{Free})^{b_i}}{1 + (k_i [ANS]_{Free})^{b_i}} \quad (XIII)$$

where  $C_i$  are the maximum concentration of ANS bound to lipids,  $k_i$  are the different association constants,  $b_i$  are parameters that give information of the cooperativity of the processes and  $n$  are the different binding sites of ANS to the sample.

To determine the variation of the surface potential in the membranes caused by *cyt c* incorporation, values of the different  $k_i$  obtained from equation XIII were used in equation XIV.

$$\Delta\Psi_{\text{cyt}} = \frac{RT}{F} \text{Ln} \left( \frac{\frac{1}{n} \sum_{i=1}^n k_i}{k_0} \right) \quad (\text{XIV})$$

where  $R$ ,  $T$  and  $F$  are the universal constant of gases, the temperature and the Faraday constant, respectively;  $k_i$  are the apparent association constants obtained in the samples with *cyt c*,  $k_0$  is the apparent association constant of the liposomes without *cyt c* and  $n$  is the number of different binding sites.

### IV.3.1.3. Surface potential determination experiments

For each surface potential determination a minimum of three blanks (liposomes without protein) and five samples (liposomes with protein) were needed to obtain representative values. Samples were incubated with the desired volume of *cyt c* during 30 minutes under continuously stirring and constant temperature of 24 °C. Blanks were incubated with the same volume of buffer without protein and in the same conditions that the samples. With this procedure the dilution errors were taken into account.

Experiments were performed monitoring the fluorescence emission of ANS as a function of the ANS concentration in the cuvette at 24 °C.

### IV.3.2. Determination of $T_m$ of lipid mixtures

1,6-Diphenil-1,3,5-hexatriene was used to determine transition temperatures in liposomes of different membrane compositions. Its molecular structure is represented in Figure 33.

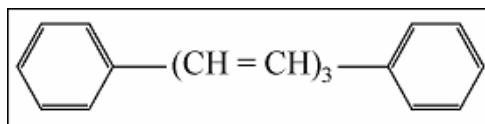


**Figure 33.** DPH molecular structure.

DPH is a classical fluorescent probe to monitor membrane hydrophobic regions. Its fluorescence in polar regions is nearly zero. Its location in membranes could be parallel to the hydrocarbon chains or perpendicular to them between the two monolayers that compound the liposome. DPH absorption and emission transition dipoles are aligned approximately parallel to its long molecular axis. So, it is highly fluorescent in absence of rotational motions; if the membrane fluidity is increased, the probe begins to move and the fluorescence decreases (such is the case of the transition between gel state to liquid crystal in lipids that compound the bilayer in a liposome). DPH presents an excitation wavelength of 381 nm and emission wavelength of 426 nm.

DPH was dissolved in a glass tube with tetrahydrofuran to a final concentration of 100  $\mu\text{M}$ . From this stock solution was taken the desired amount to perform each experiment.

Liposomes of different compositions were prepared as described in IV.1.3. section. After that, DPH probe was added to obtain a final phospholipid-probe relationship of 650:1 (mol:mol). A minimum of 30 minutes at a temperature above the  $T_m$  of the phospholipids that form the liposome was needed to incubate the fluorescent probe. During the incubation the sample was kept out from light. Experiments were performed monitoring fluorescent anisotropy ( $r$ ) as a function of temperature.

#### IV.3.2.1. Mathematical analysis of the DPH fluorescence

Experimental data were fitted to a sigmoid curve defined by equation XV.

$$r = r_2 + \frac{(r_1 - r_2)}{1 + 10^{\left(\frac{T}{T_m} - 1\right) \cdot b}} \quad (\text{XV})$$

where  $r_1$  and  $r_2$  are the maximum and the minimum fluorescence anisotropy, respectively;  $T_m$  is the transition temperature of the phospholipid mixture and  $b$  is

assimilated to the cooperativity value of the system.  $T_m$  value could be determined as the inflection point in the data representation, as can be seen in Figure 34.

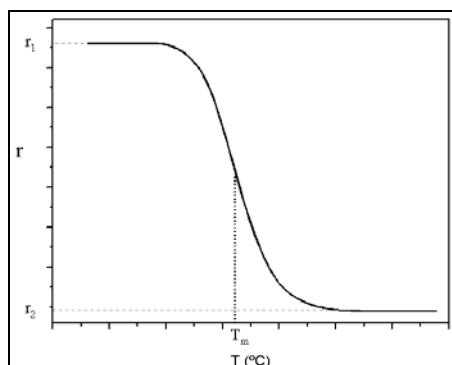


**Figure 34.** Graphic representation of fluorescence anisotropy variation with temperature.

### IV.4. SCANNING PROBE MICROSCOPIES

Scanning Probe Microscopies (SPM) are a wide group of microscopies were an ultrasharp probe scans, line by line, the surface of the sample. Although they are designed for different kind of samples, they have common parts:

- ✓ Tip
- ✓ Scanner
- ✓ Feedback system
- ✓ Output signal recording

#### IV.4.1. Tip

The tip is the probe that scans the surface of the sample. It is like an inverted tetragonal base pyramid with a height of 10  $\mu\text{m}$  and a round vertex at the top of 10 – 20 nm. Figure 35 shows a SEM image of an AFM tip (left) and its schematic representation (right).

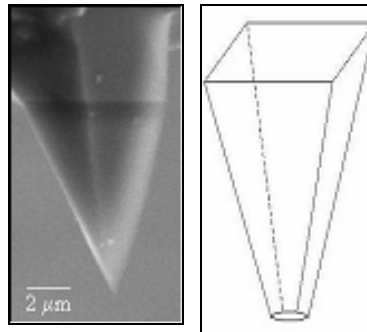


**Figure 35.** SEM image of an AFM tip and its schematic representation.

AFM tips are usually constituted of Si or  $\text{Si}_2\text{O}_3$  and can be easily functionalized with molecules (thiols, silanes, antibodies, etc).

In the AFM, the tip is at the end of a flexible lever called *cantilever* with a mean length of 100  $\mu\text{m}$ . This cantilever allows the tip oscillate at a controlled frequency. Figure 36 shows a SEM image of the tip-cantilever system.

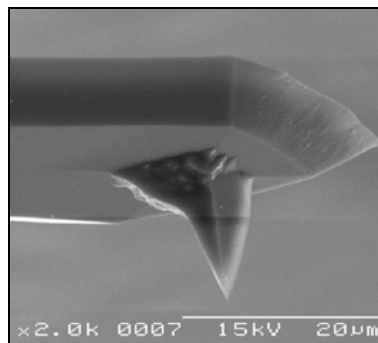


**Figure 36.** SEM image of a cantilever with a tip at its end.

A cantilever can be taken as a spring where the tip is at one of the open ends. So, mathematical treatment of forces is governed by Hooke's law:

$$F = -k \cdot x \quad (\text{XVI})$$

where  $x$  is the displacement from the origin and  $k$  the spring constant, in this case the cantilever constant. Resonant frequency of the cantilever,  $\nu_{res}$ , can be described as:

$$v_{res} = \frac{1}{2\pi} \sqrt{\frac{k}{m}} \quad (\text{XVII})$$

where  $k$  and  $m$  are the constant and mass of the cantilever, respectively. Low mass values are required to achieve a high resonant frequency, at a  $k$  constant value.

For a simple manipulation of the cantilevers, they are located at the end of a macroscopic chip. This chip is placed in a cell that serves as a support and the mass to absorb the vibration of the cantilever. A picture of a cell to scan samples in air is represented in Figure 37.

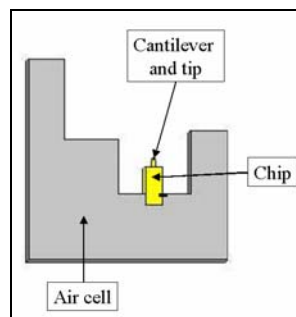


**Figure 37.** Chip with cantilever and tip placed in a cell to scan in air.

Backside of AFM cantilevers must be reflecting to detect cantilever deflection due to sample topography. Then a light beam can be reflected in this side and will allow the determination of the cantilever deflection.

#### IV.4.2. Scanner

Scanner controls the position between the sample and the tip. It is made of a piezoelectric material. Piezoelectric materials are those that suffer elastic vibrations when they are under an oscillating electric field due to the piezoelectric effect. The piezoelectric effect is the deformation property that some dielectric materials undergo when an external electric field is applied on them. Then, when an external oscillating electric field is applied to a piezoelectric material, the scanner oscillate at the same frequency that the excitation frequency of the electric field. Maximum deformation amplitude is achieved for some frequencies. These frequencies are called resonant

frequencies. In the system used in this work sample is placed on the scanner. So, the sample can be moved in X, Y and Z and in both directions. A scanner can be described as two concentric cylindrical tubes. The external one is divided in four quadrants as can be seen in Figure 38.

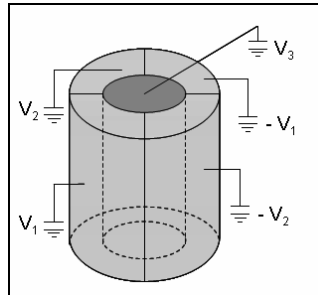


**Figure 38.** Scanner schematic representation

When voltage is applied to one of these quadrants sample is moved to this direction. If voltage is applied to the central cylinder the sample is moved in Z direction. Sample can be moved in reference to the tip position allowing an automatic scan. Scanner head is made of a magnetic material; the sample is placed on a magnetic steel disk to obtain a perfect unity between the scanner and the sample.

#### IV.4.3. Feedback system

Feedback system is a closed system between the sample and the detector. Sample position can be corrected if detection signal is achieved keeping output signal constant. Input signal is corrected to obtain a constant sample-tip distance. This process is shown in Figure 39. The lower the time needed to correct the input signal, the quicker the images can be achieved.

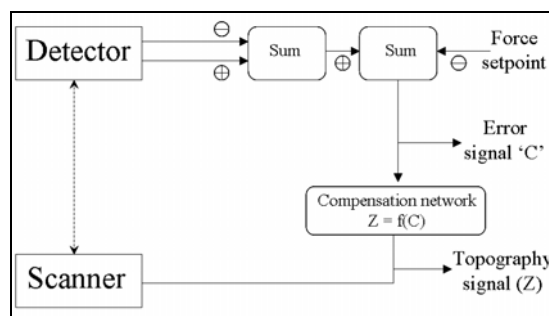


**Figure 39.** Feedback loop schema.

#### IV.4.4. Output signal register system

A computer with suitable software that acquires and processes signal of the detector achieves the microscope output signal. Usually in AFM, surface topographic images are displayed and registered.

#### IV.5. ATOMIC FORCE MICROSCOPE

Atomic Force Microscopy is one of the most used techniques of the Scanning Probe Microscopies. It was developed by Binnig and Quate in 1986 [Binnig et al., 1986]. Its lateral resolution is in the nanometric range while vertical resolution is below Å. So its vertical resolution is similar to an interferometer.

Many compounds of AFM are the same than those described in SPM but need new ones, as:

- ✓ Laser
- ✓ Photodiode

##### IV.5.1. Laser

Laser is the acronym of *Light Amplification by Stimulated Emission of Radiation*. It is a highly focalized coherent and monochromatic photon beam.

In AFM the reflecting back side of the cantilever where tip is located deflects the laser beam. This reflected laser beam strikes in a detector as can be seen in Figure 40. Variations in the deflection angle give information of the position of the tip.

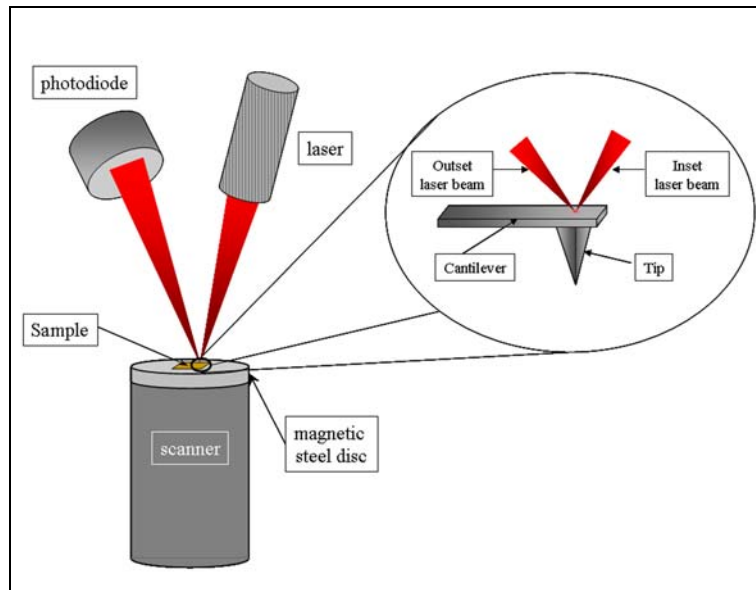


Figure 40. Laser deflection on the backside of the cantilever.

#### IV.5.2. Photodiode

The detector of the system is a photodiode. Photodiodes are diodes that transform photons from the radiation field in an electric current. A diode can be a heterounion of two semiconductors, one of *p* type (majority transporters are holes) and other of *n* type (majority transporters are electrons). When a photon incises in the photodiode it originates a hole-electron couple. Electrons migrate to the *n* zone while holes migrate to the *p* zone originating an electric current.

When the laser beam strikes in any of the four parts that compound the photodiode, incidence point is determined as a difference in signals measured by them. This situation is shown in Figure 41.

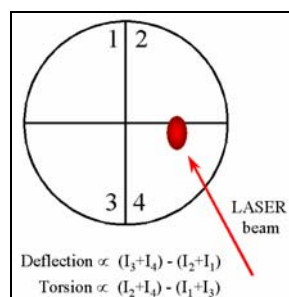


Figure 41. Incidence laser spot in the photodiode.

### IV.5.3. AFM standard scanning modes

AFM can work under three main scanning modes:

- ✓ Contact mode
- ✓ Non contact mode
- ✓ Tapping<sup>®</sup> mode

#### IV.5.3.1. Contact mode

First AFM worked in contact mode [Binnig et al., 1986]. In this mode tip is in continuous contact with the surface of the sample, so force on the tip is repulsive with mean values of  $10^{-9}$  N. Tip position is determined by cantilever angular deflection while it scans the surface due to topographic irregularities of the sample. Two different contact modes exist: constant height mode, where the scanner has a fixed position and angular deflection of the cantilever achieves the topographic image. Constant height mode is usually used on flat surfaces where the feedback system is not needed for a correct image processing. The other mode is the constant force mode, where the load force is kept constant. Topographic irregularities bend the cantilever that reflects the laser beam in a different angle than in flat sample areas. This angle difference is detected by the photodiode and compared with a continuous one from the feedback system. Then feedback system applies enough potential to the scanner to adjust its position to compensate the cantilever deflection. Position of the scanner shows the topographic image while the current applied to the scanner is called *deflection* image and can be achieved as the same time than the topographic image.

One trouble with this mode is that it can be destructive with soft samples. While tip scans the sample surface it can drag parts of the surface away. If sample is not drag away this mode can deforms it and the height of the structures in the topography image can be erroneous. This effect can be seen in Figure 42.

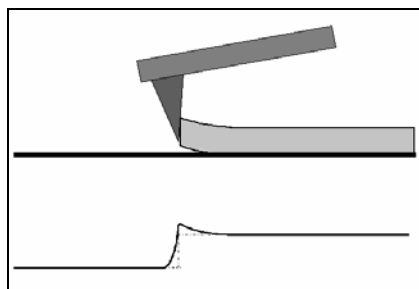


**Figure 42.** Contact mode of a soft sample. Below can be seen the section of the topographic image.

To minimize this effect tips used have low cantilever constant and force applied must be as low as possible. Besides, when low forces are applied a new effect on the tip appears. When a sample is scanned in air with humidity different to zero a thin water film appears adsorbed on it. In this situation, if tip is bringing near the surface, the surface tension of the water draws the tip towards the sample surface. The mean value of this capillary force depends on tip geometry, but its magnitude order is nearly 10 nN. So a limiting force that can be applied to the tip in air exists. This capillary effect disappears when the scanning is performed in aqueous solution.

#### IV.5.3.2. Non-contact mode

Non-contact mode was introduced by Martin and co-workers in 1987 [Martin et al., 1987]. In this mode tip never reach the sample surface diminishing lateral forces on the sample. It was developed to obtain more accurately imaging of soft biological samples. In this mode cantilever oscillates near its resonant frequency over the sample, typically 1-10 nm above the surface (Figure 43).

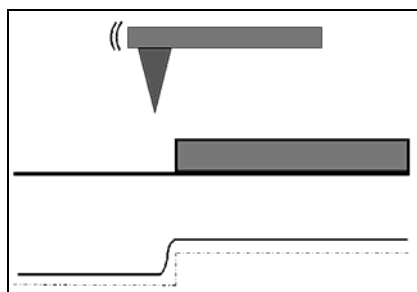


**Figure 43.** Non-contact mode of a soft sample. Below it can be seen the section of the topographic image.

Forces exerted on the tip are attractive Van der Waals forces, but they are several orders lower than the forces in contact mode. To improve the detection of these forces, the tip must be forced to oscillate. An AC detection method is used to detect the small forces between the tip and the sample by measuring the change in amplitude, phase, or frequency of the oscillating cantilever in response to force gradients from the sample. Topographic image resolution is degraded in this mode due to the detection of small forces. Non-contact mode erase lateral deformation of soft samples produced in contact mode, but a new problem appears. If something, a drop of water, is adsorbed in the surface, the non-contact mode detects it as a part of the surface. This effect is shown in Figure 44.

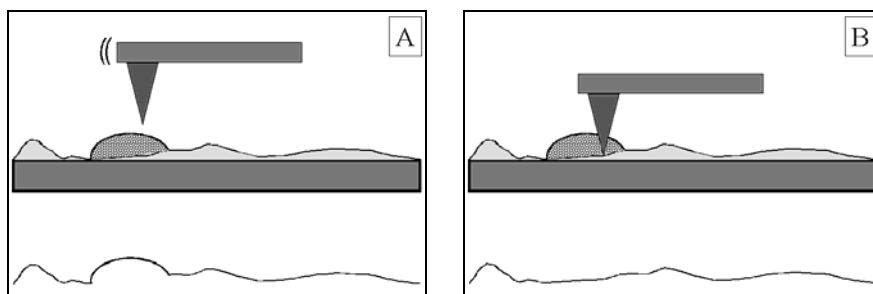


**Figure 44.** A) Non-contact mode and B) contact mode scanning of an adsorbed droplet. Below it can be seen the sections of the topographic images.

#### IV.5.3.3. Tapping<sup>®</sup> mode

Tapping<sup>®</sup> mode or intermittent contact mode was introduced by Zhong in 1993 [Zhong and Inness, 1993]. This mode is very similar to non-contact mode but the amplitude of oscillation allows the tip touch the sample surface, as can be seen in Figure 45.

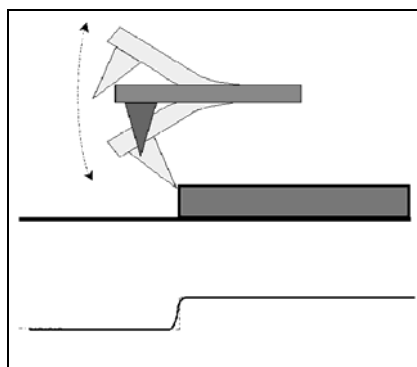


**Figure 45.** Schematic representation of the intermittent contact mode. Below it can be seen the section of the topographic image.

Intermittent contact mode allows high resolution topographic imaging of sample surfaces that are easily damaged or difficult to image by other AFM modes, as contact mode. This mode overcomes problems associated with friction, adhesion, electrostatic forces, and other difficulties alternately placing tip in contact with the surface, to provide high resolution, and then lifting the tip off from the surface to avoid dragging the tip across the surface. The cantilever where the tip is located is forced to oscillate while the tip is shifted to and fro the sample surface. This oscillation is near the resonant frequency of the cantilever with high amplitude (typically greater than 20 nm). Oscillation amplitude is maintained constant by the feedback system modifying the scanner position to apply the low possible force on the sample. If oscillation amplitude is fixed and the feedback system is turn off the force applied to the sample is not the lower that can be applied. When a protrusion appears in the sample, force applied is greater because the cantilever is forced to oscillate with amplitude lower than the needed to exert the minimum force. When a valley appears in the sample, force applied is not enough to reach the sample surface. By contrast, when the feedback system is turn on, scanner position is moved upwards or towards the sample when a protrusion or a valley appears in the scanning, respectively. This effect is shown schematically in Figure 46.

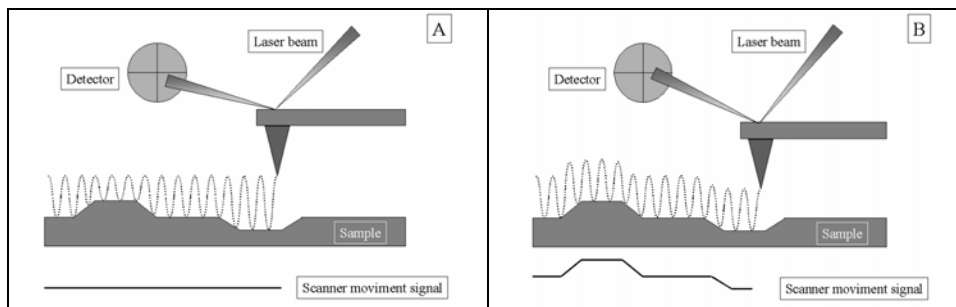


**Figure 46.** Effect of feedback system A) turn off and B) turn on in the intermittent contact mode.

In comparison with non-contact mode, intermittent contact mode provides better resolution images as well as in wide topographic scans and with many different heights. In comparison with contact mode, intermittent contact mode prevents the lateral forces (friction forces) between the tip and the sample. This is due to the tip only touch the surface in the maximum amplitude of the oscillation, retracts from the surface and move to the next point without scratching laterally the sample.

### IV.5.4. AFM experimental methodology

Samples were prepared as described in section IV.1.5. and incubated on a freshly cleaved mica surface. Mica was glued onto a Teflon disc by a water insoluble epoxy. This Teflon disc was glued onto a steel disc and then mounted onto the piezoelectric scanner. After allowing vesicles to adsorb at room temperature mica surface was gently washed with  $\text{Ca}^{2+}$  free buffer. Instrument was equipped with a “J” scanner (120  $\mu\text{m}$ ) and Tapping<sup>®</sup> mode fluid cell was extensively washed with ethanol, water and dried under a  $\text{N}_2$  stream before each experiment. Set point was continuously adjusted during the imaging to minimize the force applied. Prior to imaging the sample, the tip-sample pair was thermally stabilized. Scan rate was always less than 1.5 Hz with a scanning angle of  $0^\circ$ . All images were processed using Digital Instruments software.



